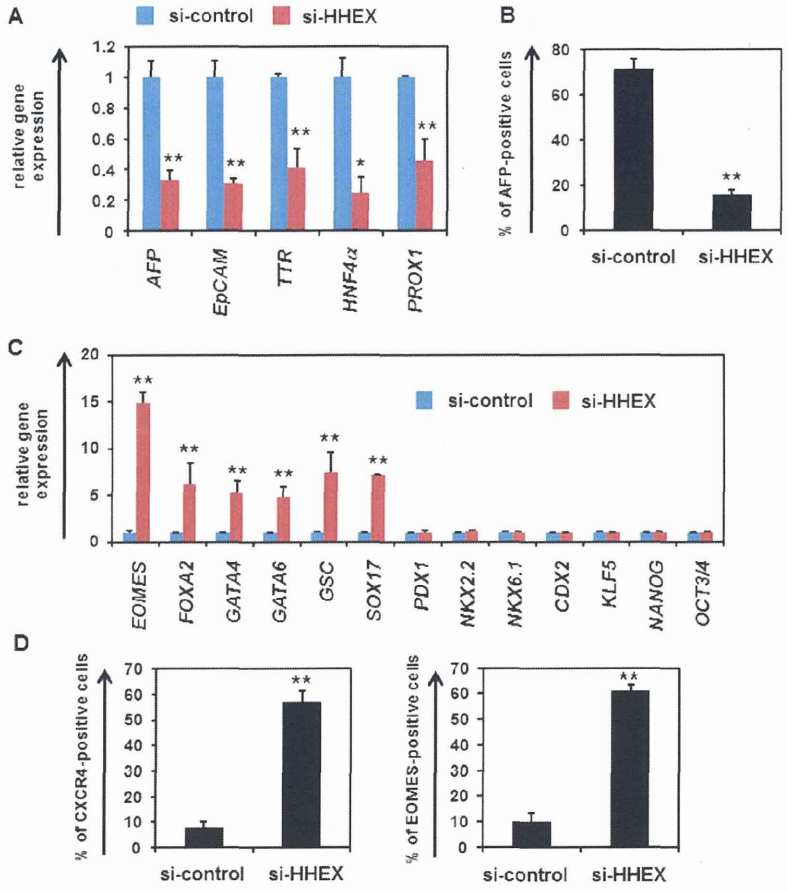

Figure 1. The expression levels of DE markers in the si-HHEX-transfected cells were upregulated in hepatoblast differentiation from DE cells. (**A**) hESCs (H9) were differentiated into DE cells according to the protocol described in the *Materials and Methods* section. The DE cells were transfected with 50 nM si-control or si-HHEX on day 4, and cultured in the medium containing 20 ng/ml BMP4 and 20 ng/ml FGF4 until day 9. On day 9, the gene expression levels of hepatoblast markers (*AFP*, *EpCAM*, *TTR*, *HNF4α*, and *PROX1*) in si-control- or si-HHEX-transfected cells were examined by real-time RT-PCR. The gene expression levels in the si-control-transfected cells were taken as 1.0. (**B**) On day 9, the percentage of AFP-positive cells was measured by using FACS analysis to examine the hepatoblast differentiation efficiency. (**C**) The gene expression levels of DE (*EOMES*, *FOXA2*, *GATA4*, *GATA6*, *GSC*, and *SOX17*), pancreatic (*PDX1*, *NKX2.2*, and *NKX6.1*), intestinal (*CDX2* and *KLF5*), and pluripotent markers (*NANOG* and *OCT3/4*) in the si-control- or si-HHEX-transfected cells were examined by real-time RT-PCR. The gene expression levels in the si-control-transfected cells were taken as 1.0. (**D**) On day 9, the percentage of cells positive for the DE markers (CXCR4 and EOMES) was examined by using FACS analysis. All data are represented as means ± SD ($n = 3$). *$p<0.05$, **$p<0.01$.
doi:10.1371/journal.pone.0090791.g001

Each 5′ UTR of the human EOMES was cloned into the promoter region of the pGL3-Basic vector (Promega) using KpnI and NcoI restriction sites. In addition, the 400 bp region around the HHEX response element (HRE) was amplified by using the following primers: 5′-CCTGCTAGCGTTCTCTGGTACTTTTCAAAATGGTGC-3′ and 5′-GAAAACTAGTATGCGCCTGTGCAAGGGAATAGAATCAG-3′. The 400 bp region around the HRE was cloned into the enhancer region of each of pGL3-EOM-5UTR1000 and pGL3-EOM-5UTR4000 using XbaI restriction site to generate pGL3-EOM-5UTR1000 containing the region around the HRE (p5′ EOM-Luc) and pGL3-EOM-5UTR4000 containing the region around the HRE (pLong-5′ EOM-Luc).

To generate pGL3-EOM-5UTR1000 containing the region which has a mutated HRE reporter construct (p5′ EOM-mut-Luc), the following base substitutions were introduced into the 400 bp region around the HRE: 5′-TCCCAATTAAAATC-3′ to 5′-TCC***AGCTGAC***AATC-3′. PCR products were cloned into the enhancer region of pGL3-EOM-5UTR1000 using XbaI restriction site.

Luciferase Reporter Assays

HeLa cells were transfected with each of the firefly luciferase reporter plasmids described above (p5′ EOM-Luc or p5′ EOM-mut-Luc) or control plasmids, pGL3-Basic vector plasmids (pControl-Luc), by using Lipofectamine 2000 (Invitrogen)-mediated gene transfection according to the manufacturer's instructions. HeLa cells were seeded at a density of 2.0×10^5 cells/well in 24-well tissue culture plates, and cultured for 24 hours before transfection. HeLa cells were transfected with 333 ng/well of each firefly luciferase reporter plasmids (pControl-Luc, p5′ EOM-Luc, or p5′ EOM-mut-Luc), 333 ng/well of HHEX expression plasmids (pHMEF5-HHEX [13]) or blank expression plasmids (pHMEF5), and 333 ng/well of internal control plasmids (pCMV-

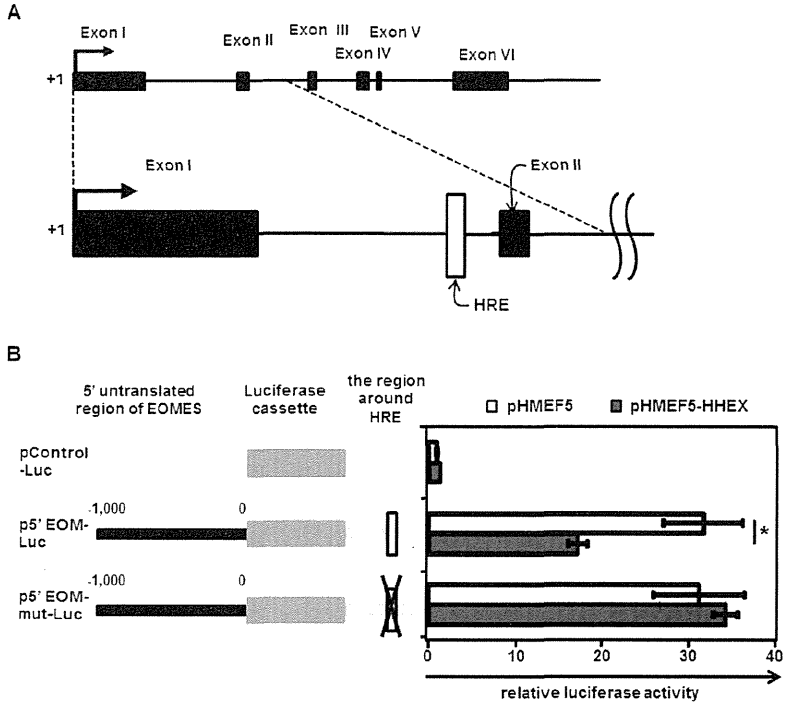

Figure 2. HHEX suppresses EOMES expression by binding to the HRE located in the first intron of EOMES. (**A**) An overview of the EOMES mRNA precursor and the location of the putative HRE are presented. The HRE is located in the first intron of EOMES. (**B**) Luciferase reporter assays were performed to examine the regulation of EOMES expression by HHEX. HeLa cells were cotransfected with both firefly luciferase reporter plasmids (pControl-Luc, p5′ EOM-Luc, or p5′ EOM-mut-Luc) and effecter plasmids (control plasmids (pHMEF5) or HHEX expression plasmids (pHMEF5-HHEX)). The details of the luciferase reporter assays are described in the *Materials and Methods* section. The luciferase activities in the pControl-Luc- and pHMEF5-cotransfected cells were taken as 1.0. All data are represented as means ± SD ($n=3$). *, $p<0.05$.
doi:10.1371/journal.pone.0090791.g002

Renilla luciferase), and cultured for 72 hours. The luciferase activities in the cells were measured by using Dual Luciferase Assay System (Promega) according to the manufacturer's instructions. Firefly luciferase activities in the cells were normalized by the measurement of renilla luciferase activities. The luciferase activity in the cells cotrasfected with pControl-Luc and pHMEF5 was assigned a value of 1.0.

siRNA Transfection

Knockdown of HHEX or EOMES was performed using a specific small interfering RNA (siRNA) fourplex set targeted to HHEX or EOMES, respectively (Darmacon SMARTpool) (Thermo Fisher Scientific). Si-Control (Darmacon siGENOME Non-Targeting siRNA Pool) (Thermo Fisher Scientific) was used as a control. Lipofectamine RNAiMAX (Invitrogen)-mediated gene transfection was used for the reverse transfection according to the manufacturer's instructions. The hESC-derived DE cells on day 4 were transfected with 50 nM of siRNA for 6 hours by reverse transfection.

Immunohistochemistry

The hESC-derived cells were fixed with methanol or 4% PFA. After blocking with PBS containing 1% BSA (Sigma), 0.2% Triton X-100 (Sigma), and 10% FBS, the cells were incubated with primary antibody at 4°C overnight, followed by incubation with a secondary antibody that was labeled with Alexa Fluor 488 (Invitrogen) at room temperature for 1 hour. All the antibodies are listed in **Table S2 in File S2**.

Western Blotting Analysis

The hESC-derived cells were homogenized with lysis buffer (20 mM HEPES, 2 mM EDTA, 10% glycerol, 0.1% SDS, 1% sodium deoxycholate, and 1% Triton X-100) containing a protease inhibitor mixture (Sigma). After being frozen and thawed, the homogenates were centrifuged at 15,000 *g* at 4°C for 10 minutes, and the supernatants were collected. The lysates were subjected to SDS-PAGE on 7.5% polyacrylamide gel and were then transferred onto polyvinylidene fluoride membranes (Millipore). After the reaction was blocked with 1% skim milk in TBS containing 0.1% Tween 20 at room temperature for 1 hour, the membranes were incubated with anti-human HHEX, EOMES, or β-actin antibodies at 4°C overnight, followed by reaction with horseradish peroxidaseconjugated anti-rabbit IgG or anti-mouse IgG antibodies at room temperature for 1 hour. The band was visualized by ECL Plus Western blotting detection reagents (GE Healthcare) and the signals were read using an LAS-4000 imaging system (Fuji Film). All the antibodies are listed in **Table S2 in File S2**.

Results

Obstruction of Hepatoblast Differentiation by HHEX Knockdown Results in Upregulation of the Expression Levels of DE Markers

It is known that HHEX plays an important role in hepatoblast differentiation [11–12–14]. We have previously reported that HHEX overexpression promoted hepatoblast differentiation from

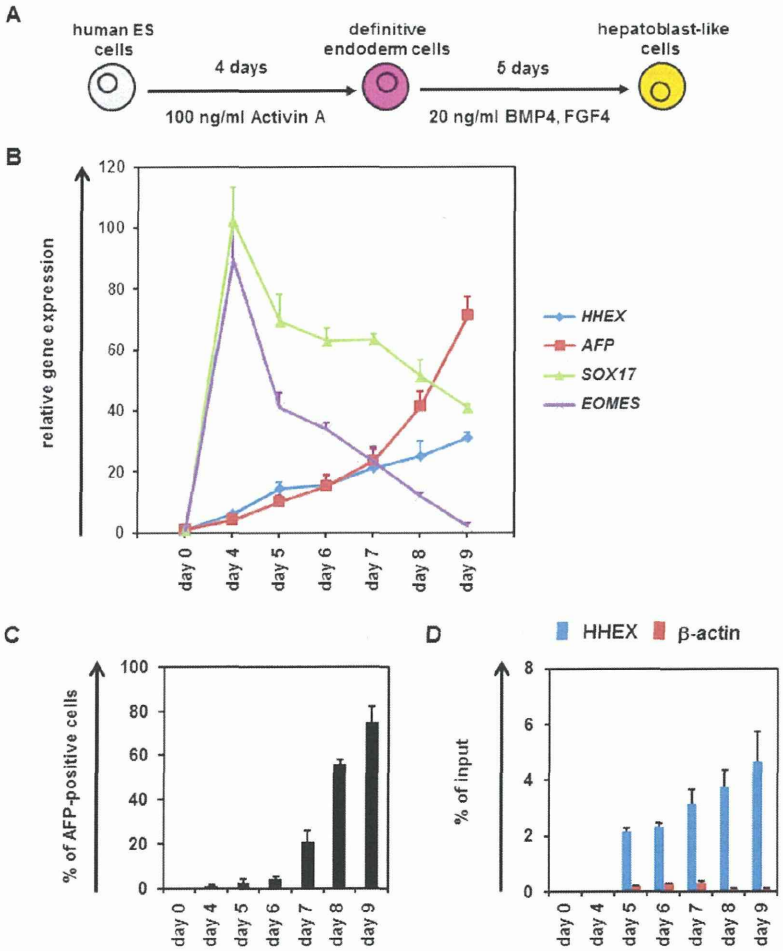

Figure 3. Temporal analysis of endogenous gene expression levels of EOMES and HHEX in hepatoblast differentiation from hESCs. (**A**) The schematic protocol for hepatoblast differentiation from hESCs (H9) is shown. (**B**) The temporal gene expression levels of *HHEX, AFP, SOX17* and *EOMES* were examined by real-time RT-PCR in hepatoblast differentiation. The gene expression levels in undifferentiated hESCs were taken as 1.0. (**C**) To examine the hepatoblast differentiation efficiency, the percentage of AFP-positive cells was measured by FACS analysis. (**D**) The HHEX protein-binding frequencies of the regions around the HRE of the EOMES gene and a negative control gene (β-ACTIN) were measured by ChIP-qPCR analysis. The results are presented as the percent input of anti-HHEX samples compared with those of anti-IgG samples. All data are represented as means ± SD ($n = 3$).

doi:10.1371/journal.pone.0090791.g003

the hESC-derived DE cells [13]. To confirm the importance of HHEX in hepatoblast differentiation, a loss of function assay of HHEX was performed by using siRNA-mediated HHEX knockdown. We confirmed the knockdown of HHEX expression in the hESC-derived DE cells that has been transfected with si-HHEX (**Fig. S1 in File S1**). The gene expression levels of hepatoblast markers in the si-HHEX-transfected cells were significantly downregulated as compared with those in the si-control-transfected cells (**Fig. 1A**). In addition, the percentage of alpha-fetoprotein (AFP; a hepatoblast marker)-positive cells was decreased by HHEX knockdown on day 9 (**Fig. 1B**). These results suggest that hepatoblast differentiation is prevented by HHEX knockdown, demonstrating that HHEX plays an important role in hepatoblast differentiation from DE cells. To characterize the si-HHEX-transfected cells on day 9, the gene expression levels of DE, pancreatic, intestinal, and pluripotent markers were examined (**Fig. 1C**). Interestingly, the gene expression levels of DE markers were significantly upregulated by HHEX knockdown, although those of pancreatic, intestinal, and pluripotent markers were not changed by HHEX knockdown. Furthermore, the percentage of DE marker (CXCR4 and EOMES)-positive cells was increased by HHEX knockdown (**Fig. 1D**). In addition, the percentage of AFP-positive cells or *EOMES* expression level was decreased or increased, respectively, by HHEX knockdown not only in the DE cells (day 4) but also in the cells starting to commit to hepatoblast (day 5–7) (**Fig. S2 in File S1**). This suggested that HHEX knockdown inhibits hepatoblast differentiation but does not simply change the number of the DE cells. These results suggest that the inhibition of HHEX expression during hepatoblast differentiation results in an increase of DE cells, but not pancreatic, intestinal, or undifferentiated cells.

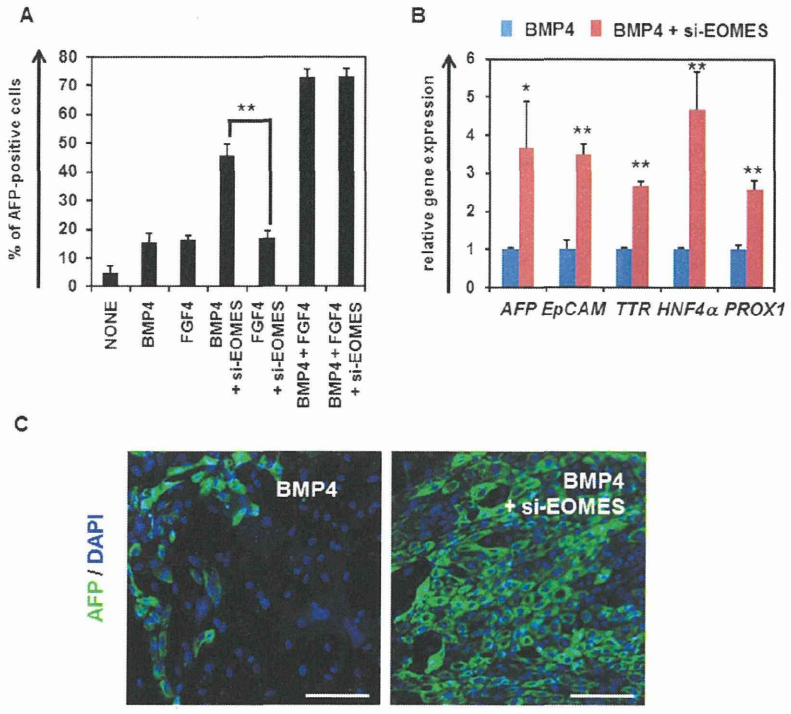

Figure 4. Hepatoblast differentiation was promoted by knockdown of EOMES in the presence of BMP4. (**A**) The hESCs (H9) were differentiated into the DE cells according to the protocol described in the *Materials and Methods* section. The hESC-derived DE cells were transfected with 50 nM si-control or si-EOMES on day 4, and then cultured with the medium containing BMP4 or FGF4. The percentage of AFP-positive cells was examined by FACS analysis on day 9. (**B**) The gene expression levels of hepatoblast markers (*AFP*, *EpCAM*, *TTR*, *HNF4α*, and *PROX1*) were measured by real-time RT-PCR on day 9. The gene expression levels in si-control-transfected cells were taken as 1.0. (**C**) The si-control- or si-EOMES-transfected cells were subjected to immunostaining with anti-AFP (green) antibodies. Nuclei were counterstained with DAPI (blue). The bar represents 50 μm. All data are represented as means ± SD ($n=3$). *$p<0.05$, **$p<0.01$.
doi:10.1371/journal.pone.0090791.g004

HHEX Directly Represses EOMES Expression

Because the gene expression level of *EOMES* was most increased by HHEX knockdown in hepatoblast differentiation, we expected that EOMES might be directly regulated by HHEX. The putative HHEX-binding site (HHEX response element (HRE)) [22] was found in the first intron of EOMES as shown in **Figure 2A**. To investigate whether HHEX could directly repress EOMES transcription, luciferase reporter assays were performed. The reporter plasmids that contain a 5′ untranslated region (UTR) of EOMES (**Fig. S3 in File S1**) and the first intron of EOMES were generated because the putative HHEX-binding site was observed in the first intron of EOMES. The luciferase reporter assays showed that p5' EOM-Luc, which contains the wild-type HRE, mediates significant repression of luciferase activity by HHEX overexpression, whereas p5' EOM-mut-Luc, which contains a mutant HRE, mediates similar luciferase activity even in the presence of HHEX (**Fig. 2B**). These results indicated that HHEX represses EOMES expression through the HRE located in the first intron of EOMES.

Endogenous Temporal Gene Expression Analysis of HHEX and EOMES in Hepatic Specification

To examine the relationship between HHEX and EOMES in hepatic specification, the temporal gene expression patterns of *HHEX* and *EOMES* were examined in hepatoblast differentiation from hESCs (**Fig. 3A**). In DE differentiation (from day 0 to 4), the gene expression levels of *EOMES* and *SOX17* were increased, although those of *HHEX* and *AFP* did not change (**Fig. 3B**). In the hepatic specification process (from day 5 to 9), the gene expression levels of *HHEX* and *AFP* began to be upregulated on day 5, and continued to increase until day 9. On the other hand, the gene expression levels of *EOMES* and *SOX17* started to decrease on day 5, and continued to decrease until day 9. We confirmed that the percentage of CXCR4-positive cells was 95.2±2.2% on day4. In addition, we confirmed that few AFP-positive cells were observed on day 5, and that the percentage of AFP-positive cells continuously increased until day 9 (**Fig. 3C**). To examine whether HHEX binds to the HRE located in the first intron of EOMES, ChIP-qPCR analysis of hepatoblast differentiation from hESCs was performed (**Fig. 3D**). HHEX bound to the HRE located in the first intron of EOMES on day 5, when the hepatic specification began. The amount of HHEX binding to that site continued to increase until day 9. These results suggest that HHEX binds to HRE located in the first intron of EOMES in hepatic specification from the DE cells.

EOMES Knockdown Promotes Hepatic Specification in the Presence of BMP4

To examine the function of EOMES in hepatoblast differentiation, EOMES was knocked down in the DE cells in the presence of BMP4 or FGF4. We confirmed the knockdown of EOMES expression in the hESC-derived DE cells that has been transfected with si-EOMES (**Fig. S4 in File S1**). Although the percentage of AFP-positive cells was increased by EOMES knockdown in the

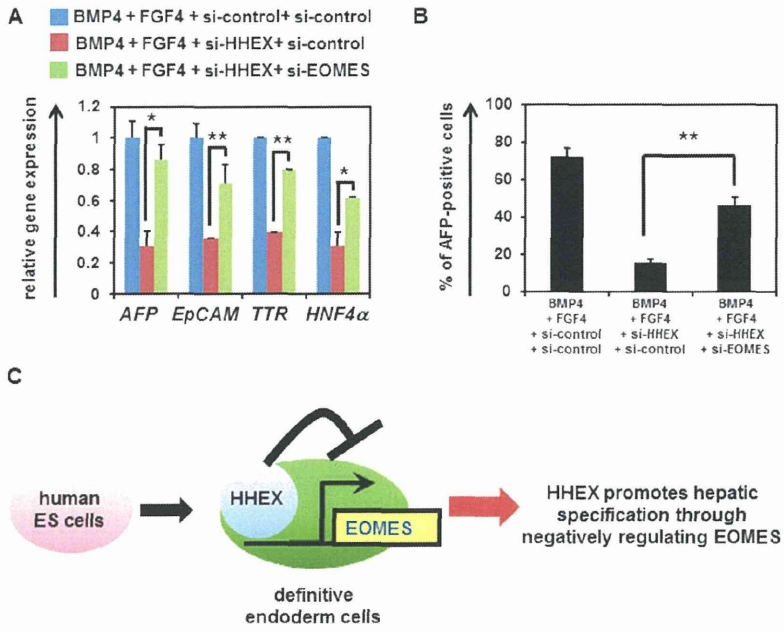

Figure 5. Hepatoblast differentiation is inhibited by EOMES, which functions downstream of HHEX. (**A**) The hESCs (H9) were differentiated into the DE cells according to the protocol described in the *Materials and Methods* section. The hESC-derived DE cells were transfected with 50 nM si-control, si-EOMES, or si-HHEX on day 4, and then cultured with the medium containing BMP4 and FGF4. The gene expression levels of hepatoblast markers (*AFP*, *EpCAM*, *TTR*, and *HNF4α*) were measured by real-time RT-PCR on day 9. The gene expression levels in si-control- and si-HHEX-transfected cells were taken as 1.0. (**B**) The percentage of AFP-positive cells was examined by FACS analysis on day 9. All data are represented as means ± SD ($n=3$). *$p<0.05$, **$p<0.01$. (**C**) HHEX promotes the hepatic specification from the hESC-derived DE cells by negatively regulating EOMES expression. A model of the hepatic specification from the hESC-derived DE cells by HHEX is presented. In the hESC-derived DE cells, HHEX represses EOMES expression. In this way, HHEX promotes the hepatic specification from the hESC-derived DE cells.
doi:10.1371/journal.pone.0090791.g005

presence of BMP4, it was not changed by EOMES knockdown in the presence of FGF4 (**Fig. 4A**). In addition, EOMES knockdown did not affect the percentage of AFP-positive cells in the presence of both FGF4 and BMP4. This might have been because the endogenous *EOMES* expression level was already sufficiently suppressed under the existence of FGF4 (**Fig. S5 in File S1**). To further investigate the function of EOMES in hepatoblast differentiation, gene expression and immunohistochemical analyses of hepatoblast markers were performed in si-EOMES-transfected cells. The gene expression levels of hepatoblast markers in si-EOMES-transfected cells were upregulated as compared with those in si-control-transfected cells (**Fig. 4B**). Consistently, the immunohistochemical analysis of AFP showed that EOMES knockdown upregulated the expression levels of AFP (**Fig. 4C**). In addition, EOMES knockdown increased the percentage of AFP-positive cells not only in the DE cells (day 4) but also in the cells starting to commit to hepatoblast (day 5–7) (**Fig. S6 in File S1**). This suggested that EOMES knockdown promotes hepatoblast differentiation but does not simply change the number of the DE cells. These results suggest that hepatic specification from the DE cells is promoted by EOMES knockdown depending on the existence of BMP4.

EOMES Functions Downstream of HHEX in the Hepatic Specification from the DE Cells

To examine whether EOMES functions downstream of HHEX in the hepatic specification from the DE cells, both HHEX and EOMES were knocked down in the DE cells, and then the gene expression profiles of hepatoblast markers were analyzed. The gene expression levels of hepatoblast markers were upregulated in both si-HHEX- and si-EOMES-transfected cells as compared with those in si-HHEX-transfected cells (**Fig. 5A**). Furthermore, the percentage of AFP-positive cells was also increased by double-knockdown of HHEX and EOMES (**Fig. 5B**). These results suggest that EOMES knockdown could promote the hepatic specification from the DE cells by HHEX knockdown. In conclusion, EOMES exerts downstream of HHEX in the hepatic specification from the DE cells.

Discussion

The purpose of this study was to identify and characterize the target genes of HHEX in hepatic specification from DE to elucidate the functions of HHEX in this process. We clearly demonstrated that the expression of EOMES is directly suppressed by HHEX, and that EOMES is one of the crucial target genes of HHEX in the hepatic specification from the hESC-derived DE cells. We also showed that EOMES knockdown in the hESC-derived DE cells could rescue the si-HHEX-mediated inhibition of hepatic specification. Our findings indicate that promotion of the hepatic specification by HHEX in the hESC-derived DE cells would be mainly mediated by the repression of EOMES expression (**Fig. 5C**).

To explore direct target genes of HHEX in the hepatic specification, EOMES knockdown experiments were conducted (**Fig. 1**). The luciferase reporter assays (**Fig. 2B**) and ChIP-qPCR (**Fig. 3C**) indicated that HHEX represses EOMES expression by binding to the first intron of EOMES containing a putative HRE. It might be expected that HHEX recruits co-repressor proteins to

repress EOMES expression because HHEX could negatively regulate the expressions of target genes such as *vascular endothelial growth factor (Vegf)* and *vascular endothelial growth factor receptor-1 (Vegfr-1)* by forming the co-repressor protein complexes [23–25]. Previous studies demonstrated that HHEX has three main domains, a repression domain, a DNA-binding domain, and an activation domain [26], and thus exerts both positive and negative effects on the target gene expressions. Taken together, these findings suggested that HHEX would repress EOMES expression through the function of its repression domain.

The results in **figure 4A** demonstrate that EOMES knockdown promoted hepatic specification in the presence of BMP4, but not FGF4. Because it was previously reported that FGF4 could induce the expression level of HHEX in the DE cells [27], FGF4 treatment in the DE cells would lead to downregulation of EOMES expression via the regulation of HHEX expression. Therefore, HHEX and EOMES might exert in the downstream of FGF4 in the hepatic specification. In addition, both BMP4 and FGF4 are necessary for hepatic specification (**Fig. 4A**). However, the functions of BMP4 in hepatic specification and the synergistic effect of BMP and FGF have not been sufficiently elucidated, and will need to be resolved in future studies.

Simultaneous knockdown of HHEX and EOMES in the hESC-derived DE cells led to rescue of the HHEX-mediated inhibition of the hepatic specification (**Fig. 5**). These results suggested that the majority of functions in the hepatic specification by HHEX may be caused by the repression of EOMES expression. EOMES is known to regulate numerous target genes related to DE differentiation, and thus the repression of EOMES expression might also promote other DE-derived lineage specifications, such as pancreatic specification. HHEX is known to regulate not only hepatic specification but also pancreatic specification [11–28]. Therefore, EOMES might also be a target gene of HHEX in pancreatic specification as well as in hepatic specification. Because the HHEX protein is known to interact with the HNF1α protein and synergistically upregulate the HNF1α target gene expression [15], it would be of interest to examine the relationship between HHEX and HNF1α in the hepatic specification from the hESC-derived DE cells. The proteomic analyses of HHEX protein in the hepatic specification from the hESC-derived DE cells might help to elucidate the functions of HHEX in this process.

Conclusions

In summary, we showed that the homeobox gene HHEX promotes the hepatic-lineage specification from the hESC-derived DE cells through the repression of EOMES expression. Previously, we reported that transduction of SOX17, HNF4α, FOXA2 or HNF1α into the hESC-derived cells could promote efficient hepatic differentiation [16–18]. The direct target genes of these genes might be identified by using the strategy described here. Furthermore, identification of the genes targeted by functional genes in the various lineage differentiation models from hESCs will promote understanding of the intricate transcriptional networks that regulate human development.

Supporting Information

File S1 Contains the following files: **Figure S1. Knockdown of HHEX in the DE cells by si-HHEX transfection. (A, B)** The hESCs (H9) were differentiated into the DE cells (day 4) according to the protocol described in *Materials and Methods* section. The DE cells were transfected with 50 nM si-control or si-HHEX on day 4. On day 6, the HHEX expression levels in si-control- or si-HHEX-transfected cells were examined by real-time RT-PCR (**A**) or Western blotting (**B**). The gene expression levels of *HHEX* in the si-control-transfected cells were taken as 1.0. All data are represented as means ± SD ($n = 3$). ** $p<0.01$. **Figure S2. The percentage of AFP-positive cells or *EOMES* expression level was decreased or increased, respectively, by HHEX knockdown. (A, B)** The hESCs (H9) were differentiated into the DE cells according to the protocol described in the *Materials and Methods* section. The DE cells were transfected with 50 nM si-control or si-HHEX on day 4, 5, 6, or 7, and cultured in medium containing 20 ng/ml BMP4 and 20 ng/ml FGF4 until day 9. On day 9, the percentage of AFP-positive cells was measured by using FACS analysis to examine the hepatoblast differentiation efficiency (**A**). Also on day 9, the gene expression levels of EOMES in si-control- or si-HHEX-transfected cells were examined by real-time RT-PCR (**B**). The gene expression levels in the si-control-transfected cells were taken as 1.0. All data are represented as means ± SD ($n = 3$). **$p<0.01$. **Figure S3. Both 1,000 bp and 4,000 bp 5′ UTR of EOMES have promoter activities.** Luciferase reporter assays were performed to examine whether 1,000 bp and 4,000 bp 5′ UTR of EOMES have promoter activity. HeLa cells were cotransfected with both 500 ng/well of firefly luciferase reporter plasmids (pControl-Luc, p5′ EOM-Luc, or pLong-5′ EOM-Luc), and 500 ng/well of internal control plasmids (pCMV-Renilla luciferase), and cultured for 72 hours. The luciferase activities in the cells were measured by using Dual Luciferase Assay System (Promega) according to the manufacturer's instructions. Firefly luciferase activities in the cells were normalized by the measurement of renilla luciferase activities. The RLU in the pControl-Luc-transfected cells was assigned a value of 1.0. All data are represented as means ± SD ($n = 3$). *, $p<0.05$. **Figure S4. Knockdown of EOMES in the DE cells by si-EOMES transfection. (A, B)** The hESCs (H9) were differentiated into the DE cells (day 4) according to the protocol described in *Materials and Methods* section. The DE cells were transfected with 50 nM si-control or si-EOMES on day 4. On day 6, the EOMES expression levels in si-control- or si-EOMES-transfected cells were examined by real-time RT-PCR (**A**) or Western blotting (**B**). The gene expression levels of *EOMES* in the si-control-transfected cells were taken as 1.0. All data are represented as means ± SD ($n = 3$). ** $p<0.01$. **Figure S5. Hepatoblast differentiation was promoted by knockdown of EOMES.** The hESCs (H9) were differentiated into the DE cells according to the protocol described in the *Materials and Methods* section. The hESC-derived DE cells were transfected with 50 nM si-control or si-EOMES on day 4, 5, 6, or 7, and then cultured in medium containing BMP4 or FGF4. The percentage of AFP-positive cells was examined by FACS analysis on day 9. All data are represented as means ± SD ($n = 3$). **$p<0.01$. **Figure S6. The *EOMES* or *HHEX* expression level was suppressed or increased, respectively, in the presence of FGF4.** The hESCs (H9) were differentiated into the DE cells according to the protocol described in the *Materials and Methods* section. The hESC-derived DE cells were cultured in medium containing BMP4 or FGF4 until day 9. The gene expression levels of *EOMES*, *HHEX*, or *AFP* in the non-treated cells (control) were taken as 1.0. All data are represented as means ± SD ($n = 3$). **$p<$ 0.01 (compared with control).
(PDF)

File S2 Contains the following files: **Table S1.** List of primers used in this study. **Table S2.** List of antibodies used in this study.
(DOC)

Acknowledgments

We thank Yasuko Hagihara, Misae Nishijima, Nobue Hirata, and Reiko Hirabayashi for their excellent technical support.

Author Contributions

Conceived and designed the experiments: HW K. Takayama MI MT K. Katayama K. Kawabata HM. Performed the experiments: HW K. Takayama MI NM. Analyzed the data: HW K. Takayama MI MT K. Katayama K. Tashiro YN FS K. Kawabata MKF HM. Wrote the paper: HW K. Takayama HM. Contributed equally to this work: HW K. Takayama.

References

1. Zaret KS, Grompe M (2008) Generation and regeneration of cells of the liver and pancreas. Science 322: 1490–1494.
2. Si-Tayeb K, Lemaigre FP, Duncan SA (2010) Organogenesis and development of the liver. Dev Cell 18: 175–189.
3. Thomson JA, Itskovitz-Eldor J, Shapiro SS, Waknitz MA, Swiergiel JJ, et al. (1998) Embryonic stem cell lines derived from human blastocysts. Science 282: 1145–1147.
4. D'Amour KA, Agulnick AD, Eliazer S, Kelly OG, Kroon E, et al. (2005) Efficient differentiation of human embryonic stem cells to definitive endoderm. Nat Biotechnol 23: 1534–1541.
5. D'Amour KA, Bang AG, Eliazer S, Kelly OG, Agulnick AD, et al. (2006) Production of pancreatic hormone-expressing endocrine cells from human embryonic stem cells. Nat Biotechnol 24: 1392–1401.
6. Si-Tayeb K, Noto FK, Nagaoka M, Li J, Battle MA, et al. (2010) Highly efficient generation of human hepatocyte-like cells from induced pluripotent stem cells. Hepatology 51: 297–305.
7. Spence JR, Mayhew CN, Rankin SA, Kuhar MF, Vallance JE, et al. (2011) Directed differentiation of human pluripotent stem cells into intestinal tissue in vitro. Nature 470: 105–109.
8. Agarwal S, Holton KL, Lanza R (2008) Efficient differentiation of functional hepatocytes from human embryonic stem cells. Stem Cells 26: 1117–1127.
9. Takayama K, Kawabata K, Nagamoto Y, Inamura M, Ohashi K, et al. (2014) CCAAT/enhancer binding protein-mediated regulation of TGFbeta receptor 2 expression determines the hepatoblast fate decision. Development 141: 91–100.
10. Bogue CW, Ganea GR, Sturm E, Ianucci R, Jacobs HC (2000) Hex expression suggests a role in the development and function of organs derived from foregut endoderm. Dev Dyn 219: 84–89.
11. Bort R, Signore M, Tremblay K, Martinez Barbera JP, Zaret KS (2006) Hex homeobox gene controls the transition of the endoderm to a pseudostratified, cell emergent epithelium for liver bud development. Dev Biol 290: 44–56.
12. Keng VW, Yagi H, Ikawa M, Nagano T, Myint Z, et al. (2000) Homeobox gene Hex is essential for onset of mouse embryonic liver development and differentiation of the monocyte lineage. Biochem Biophys Res Commun 276: 1155–1161.
13. Inamura M, Kawabata K, Takayama K, Tashiro K, Sakurai F, et al. (2011) Efficient Generation of Hepatoblasts From Human ES Cells and iPS Cells by Transient Overexpression of Homeobox Gene HEX. Mol Ther 19: 400–407.
14. Kubo A, Kim YH, Irion S, Kasuda S, Takeuchi M, et al. (2010) The homeobox gene Hex regulates hepatocyte differentiation from embryonic stem cell-derived endoderm. Hepatology 51: 633–641.
15. Tanaka H, Yamamoto T, Ban T, Satoh S, Tanaka T, et al. (2005) Hex stimulates the hepatocyte nuclear factor 1alpha-mediated activation of transcription. Arch Biochem Biophys 442: 117–124.
16. Takayama K, Inamura M, Kawabata K, Tashiro K, Katayama K, et al. (2011) Efficient and Directive Generation of Two Distinct Endoderm Lineages from Human ESCs and iPSCs by Differentiation Stage-Specific SOX17 Transduction. PLoS One 6: e21780.
17. Takayama K, Inamura M, Kawabata K, Katayama K, Higuchi M, et al. (2012) Efficient Generation of Functional Hepatocytes From Human Embryonic Stem Cells and Induced Pluripotent Stem Cells by HNF4alpha Transduction. Mol Ther 20: 127–137.
18. Takayama K, Inamura M, Kawabata K, Sugawara M, Kikuchi K, et al. (2012) Generation of metabolically functioning hepatocytes from human pluripotent stem cells by FOXA2 and HNF1alpha transduction. J Hepatol 57: 628–636.
19. Takayama K, Kawabata K, Nagamoto Y, Kishimoto K, Tashiro K, et al. (2013) 3D spheroid culture of hESC/hiPSC-derived hepatocyte-like cells for drug toxicity testing. Biomaterials 34: 1781–1789.
20. Nagamoto Y, Tashiro K, Takayama K, Ohashi K, Kawabata K, et al. (2012) The promotion of hepatic maturation of human pluripotent stem cells in 3D co-culture using type I collagen and Swiss 3T3 cell sheets. Biomaterials 33: 4526–4534.
21. Takayama K, Nagamoto Y, Mimura N, Tashiro K, Sakurai F, et al. (2013) Long-Term Self-Renewal of Human ES/iPS-Derived Hepatoblast-like Cells on Human Laminin 111-Coated Dishes. Stem Cell Reports 1: 322–335.
22. Gong R, Jiang X, Wilson CM, Hunter MP, Vasavada H, et al. (2006) Hhex is a direct repressor of endothelial cell-specific molecule 1 (ESM-1). Biochem Biophys Res Commun 346: 535–545.
23. Noy P, Williams H, Sawasdichai A, Gaston K, Jayaraman PS (2010) PRH/Hhex controls cell survival through coordinate transcriptional regulation of vascular endothelial growth factor signaling. Mol Cell Biol 30: 2120–2134.
24. Guiral M, Bess K, Goodwin G, Jayaraman PS (2001) PRH represses transcription in hematopoietic cells by at least two independent mechanisms. J Biol Chem 276: 2961–2970.
25. Swingler TE, Bess KL, Yao J, Stifani S, Jayaraman PS (2004) The proline-rich homeodomain protein recruits members of the Groucho/Transducin-like enhancer of split protein family to co-repress transcription in hematopoietic cells. J Biol Chem 279: 34938–34947.
26. Crompton MR, Bartlett TJ, MacGregor AD, Manfioletti G, Buratti E, et al. (1992) Identification of a novel vertebrate homeobox gene expressed in haematopoietic cells. Nucleic Acids Res 20: 5661–5667.
27. Morrison GM, Oikonomopoulou I, Migueles RP, Soneji S, Livigni A, et al. (2008) Anterior definitive endoderm from ESCs reveals a role for FGF signaling. Cell Stem Cell 3: 402–415.
28. Bort R, Martinez-Barbera JP, Beddington RS, Zaret KS (2004) Hex homeobox gene-dependent tissue positioning is required for organogenesis of the ventral pancreas. Development 131: 797–806.

SCIENTIFIC REPORTS

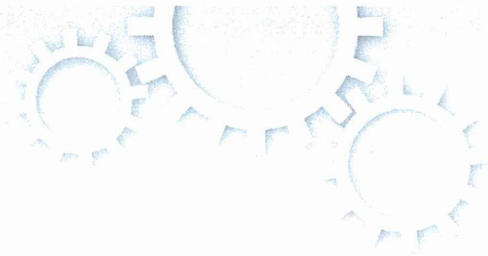

OPEN

SUBJECT AREAS:
INDUCED PLURIPOTENT STEM CELLS
EMBRYONIC STEM CELLS

Received
18 April 2013

Accepted
25 March 2014

Published
11 April 2014

Correspondence and requests for materials should be addressed to K.O. (kohnuma@vos.nagaokaut.ac.jp)

Enzyme-free Passage of Human Pluripotent Stem Cells by Controlling Divalent Cations

Kiyoshi Ohnuma[1,2], Ayaka Fujiki[3], Kana Yanagihara[3], Saoko Tachikawa[1], Yohei Hayashi[2], Yuzuru Ito[4], Yasuko Onuma[4], Techuan Chan[2], Tatsuo Michiue[2], Miho K. Furue[3] & Makoto Asashima[2,4]

[1]Top Runner Incubation Center for Academia-Industry Fusion, Nagaoka University of Technology, 1603-1 Kamitomioka, Nagaoka, Niigata 940-2188, Japan, [2]Department of Life Sciences (Biology), Graduate School of Arts and Sciences, The University of Tokyo, 3-8-1 Komaba, Meguro, Tokyo 153-8902 Japan, [3]Laboratory of Stem Cell Cultures, Department of Disease Bioresources Research, National Institute of Biomedical Innovation, 7-6-8, Saito-Asagi, Ibaraki, Osaka 567-0085, Japan, [4]Research Center for Stem Cell Engineering, National Institute of Advanced Industrial Science and Technology (AIST), Tsukuba Central 4, 1-1-1 Higashi, Tsukuba, 5 Ibaraki 305-8562, Japan.

Enzymes used for passaging human pluripotent stem cells (hPSCs) digest cell surface proteins, resulting in cell damage. Moreover, cell dissociation using divalent cation-free solutions causes apoptosis. Here we report that Mg^{2+} and Ca^{2+} control cell-fibronectin and cell-cell binding of hPSCs, respectively, under feeder- and serum-free culture conditions without enzyme. The hPSCs were detached from fibronectin-, vitronectin- or laminin-coated dishes in low concentrations of Mg^{2+} and remained as large colonies in high concentrations of Ca^{2+}. Using enzyme-free solutions containing Ca^{2+} without Mg^{2+}, we successfully passaged hPSCs as large cell clumps that showed less damage than cells passaged using a divalent cation-free solution or dispase. Under the same conditions, the undifferentiated and early-differentiated cells could also be harvested as a cell sheet without being split off. Our enzyme-free passage of hPSCs under a serum- and feeder-free culture condition reduces cell damage and facilitates easier and safer cultures of hPSCs.

Human pluripotent stem cells (hPSCs), including human embryonic stem cells (hESCs) and human induced pluripotent cells (hiPSCs), have increased the possible applications of stem cell research in biology and medicine[1–3]. Since dissociating hPSCs into single cells using divalent cation-free solution causes cell damage and death by apoptosis[4–8], hPSC passaging usually entails dissociating the cell colonies into large cell clumps using enzymes in a divalent cation-containing solution (Table 1). However, these enzymes may also induce cell damage by digesting cell-surface proteins[5,8].

To achieve enzyme-free and less damaging passage of hPSCs, we focused on the roles of Ca^{2+} and Mg^{2+} in cell-cell and cell-fibronectin binding. Physiological concentrations of Ca^{2+} regulate cell-cell binding of hPSCs mediated by E-cadherin[2,7,9,10]. On the other hand, physiological concentrations of Mg^{2+} are required for optimal, tight binding between cells and fibronectin, part of the extracellular coating matrix of hPSCs[11–15]. We therefore hypothesized that solution containing physiological concentration of Ca^{2+}, but no Mg^{2+}, could be used to passage hPSCs cultured on fibronectin-coated dishes as large cell clumps without the need for enzyme-based cell dissociation. We tested this hypothesis using our serum- and feeder-free culture medium (ESF9a) in fibronectin-coated dishes[14,16,17], allowing us to examine hPSC attachments without masking by undefined adherent factors derived from the serum and feeder cells.

Results

Dose-dependent effects of Mg^{2+} and Ca^{2+} on cell-fibronectin and cell-cell binding. The hiPSCs 253G1[18] and 201B7[2] were incubated in phosphate-buffered saline (PBS) containing various concentrations (0, 10, 100, 1000 μM) of Mg^{2+} and Ca^{2+} and then triturated to detach cells from the fibronectin-coated plates and dissociate them into cell clumps (Fig. 1a). The number of cells remaining on the dishes decreased with decreasing Mg^{2+} concentration, although the sizes of the detached hPSCs clumps increased with increasing Ca^{2+} concentration (253G1: Fig. 1b–e, 201B7: Supplementary Fig. 1ab). These results suggest that the cell-fibronectin binding depended on Mg^{2+} concentration whereas cell-cell binding of hPSCs was dependent on Ca^{2+} concentration, and that these bindings could be independently controlled without enzyme.

Table 1 | Passaging protocols for hPSC culture

Passage Protocols				Culture Conditions		References
Divalent cations	Enzymes	Manipulation	Cell clump size	Serum replacement	Coat** & feeder	
Ca^{2+}, Mg^{2+} *	Collagenase	Cutting, Scraping, Glass beads	Large	KSR,	MEF	1,27
Ca^{2+}, Mg^{2+} *	Free	Cutting	Large	KSR	MEF	5
Ca^{2+} ***	Trypsin & Collagenase	Pipetting	Large	KSR	MEF	2,6,23
Free (EDTA)	Trypsin TrypLE	Pipetting	Single cells, Large	KSR	MEF	4–6,19,28
Free (EDTA)	Free (CDB#)	Pipetting	Single cells	KSR	MEF	5
Ca^{2+}, Mg^{2+} *	Dispase, Collagenase TrypLE	Scraping, Pipetting	Large	Free	Mg, Gx, Lm, Vn, Fb, Cg, pVn, pBSP	8,14,15,20,29
Ca^{2+}, Mg^{2+} *	Free	Cutting	Large	Free	Vn	12
Free (EDTA)	Free (CDB#)	Pipetting	Small	Free	Mg, HBP	8,30
Ca^{2+}	Free	Pipetting	Large (Small)	Free	Fb	Present study

*DEME/F12 or ESF solution[16] containing Ca^{2+}, Mg^{2+}.
**MEF: mouse embryonic fibroblast feeder cells on gelatin-coated dishes, Mg: Matrigel, Gx: geltrex, Lm: laminin, Vn: vitronectin, Cg: collagen, pVn: vitronectin-derived peptide, pBSP: bone sialoprotein-derived peptide, HBP: heparin-binding peptide.
***Dissociation solution named CTK containing $CaCl_2$, trypsin, collagenase IV, and KSR[23]. KSR contains many divalent cations.
CDB: Cell dissociation Buffer (Life Technologies).

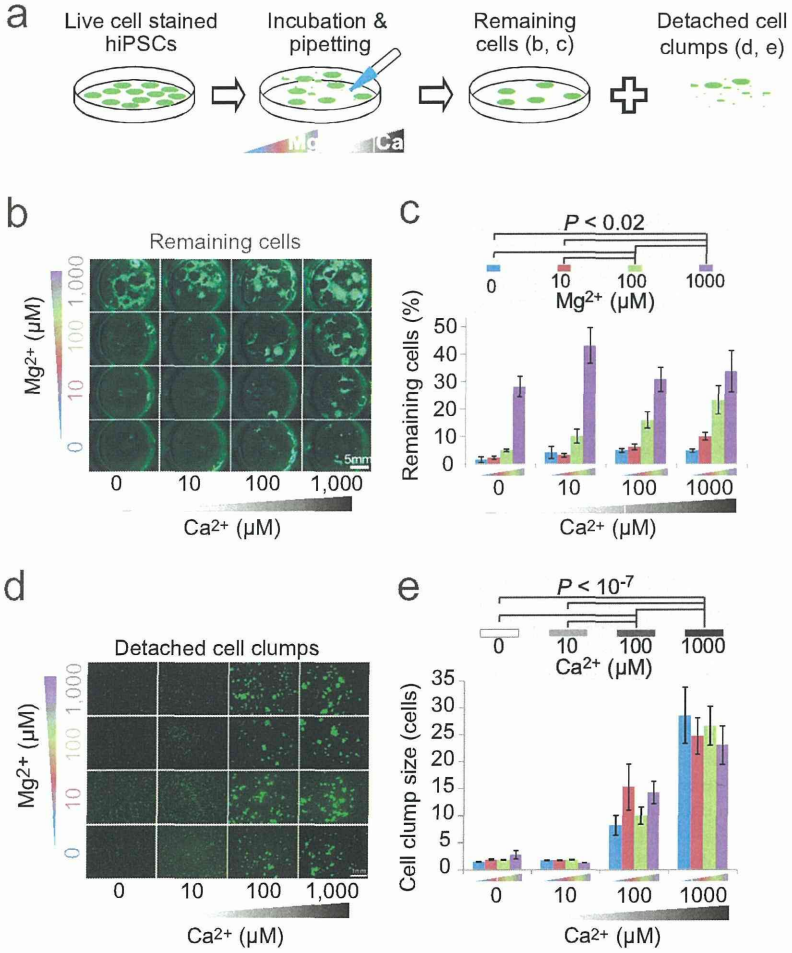

Figure 1 | Dose-dependent effects of Mg^{2+} and Ca^{2+} on cell-fibronectin and cell-cell binding. (a): Schematics of experiments. The illustrations were drawn by KO. (b–e): Fluorescent imaging (live-cell dye, Calcein-AM) of the hiPSCs (253G1) remaining on the fibronectin-coated 24-well plate (b) and the cells detached from the plate (d) after incubation and then trituration using a 1-ml pipette tip in PBS containing 0–1000 μM Ca^{2+} and Mg^{2+}. (c): Remaining-cell ratios equal the area of remaining cells divided by the area of the cells before incubation and trituration. (d): Mean cell clump size detached from the plates. Two-way ANOVA revealed no interaction effect between Ca^{2+} and Mg^{2+} concentration ((c): $P = 0.066$, mean ± SE, n = 5, (e): $P = 0.47$, mean ± SE, n = 5 experiments × 200 cells). Post-hoc Tukey's multiple comparison revealed significant differences in remaining-cell ratio between different Mg^{2+} concentrations (the same Ca^{2+} data were put together to derive the numbers and bars in (c)) and in cell clump size between different Ca^{2+} concentrations (the same Ca^{2+} data were put together to derive the numbers and bars in (e)). Scale bars are 5 mm (b), 1 mm (d).

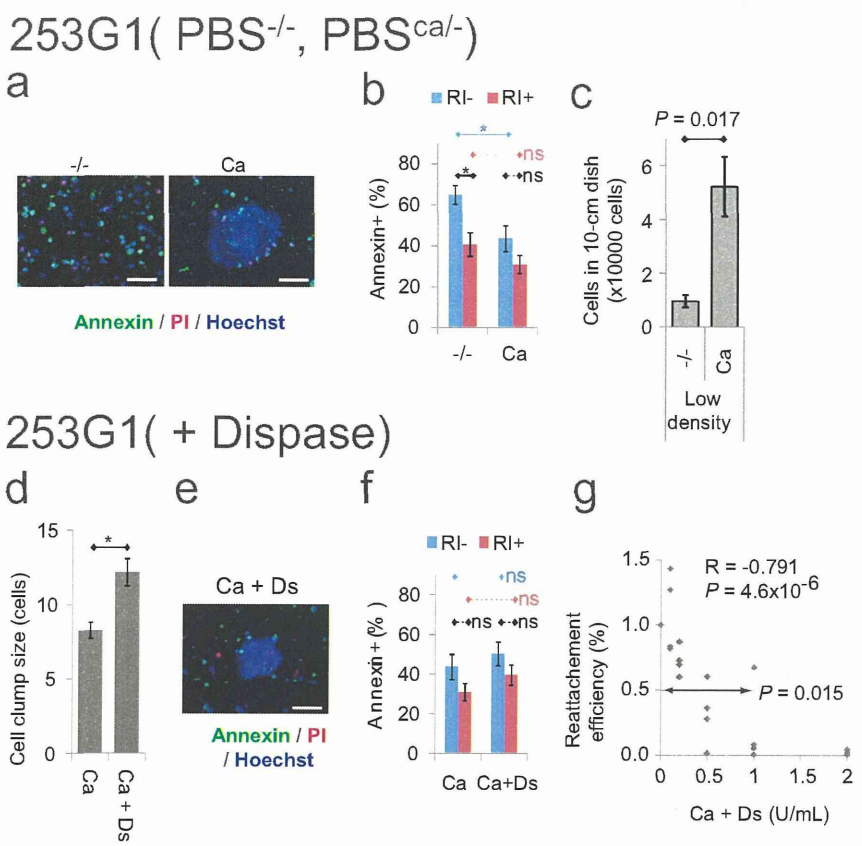

Figure 2 | Effects of dissociation without divalent cation and with dispase. (a–c): Comparison between the hiPSCs (253G1) detached and dissociated by $PBS^{-/-}$ (−/−) and those by $PBS^{ca/-}$ (Ca). (ab): Micrograph (a) and FCM analysis (b) of apoptosis marker annexin V-FITC after four hours floating culture (RI: with 5 μM ROCK inhibitor) following detachment and dissociation. The cells were stained by annexin V-FITC (green), propidium iodide (red: late apoptosis or necrosis marker), and Hoechst 33342 (blue: nuclei marker). (c): The number of cells remaining after 3 days culture in ESF9a on fibronectin-coated 10-cm dishes (the initial cell number was 1.2×10^5 cells/10-cm dish, mean ± SE, n = 5, t-test). (d–g): Effects of dispase in $PBS^{ca/-}$ for detaching and dissociating cells. (d): Mean cell clump size detached from the plates using $PBS^{ca/-}$ (Ca) and 1 U/ml dispase in $PBS^{ca/-}$ (Ca + Ds). (ef): Micrograph (e) and FCM analysis (f) of annexin V-FITC after four hours floating culture following detachment and dissociation by $PBS^{ca/-}$ or 1 U/ml dispase in $PBS^{ca/-}$. The staining were the same as (a). (g): Reattachment efficiency. The cells were digested with 0–2 U/ml dispase in $PBS^{ca/-}$ and were plated with ESF9a medium including 5 μM ROCK inhibitor. The numbers of cells were estimated using calcein-AM 1 day after plating and normalized against the $PBS^{ca/-}$ results (0 U/ml dispase). The mean value at 1 U/ml dispase was smaller than 1 ($P < 0.015$, n = 4, t-test). Pearson's correlation coefficient = −0.791, $P = 4.6 \times 10^{-6}$ t-test, from 4 independent experiments. Scale bars are 100 μm. (bdf): * $P = 0.05$, ns: not significant, n = 6, mean ± SE (bf) and * $P = 0.01$, ns: not significant, n = 4 experiments × 200 cells, mean ± SE (d), Holm's multiple comparison tests (cf. Supplementary Fig 5).

Passage of hPSCs with enzyme-free solution containing a physiological concentration of Ca^{2+} without Mg^{2+}. We tested whether the buffer solutions with Ca^{2+} and without Mg^{2+} could be used to passage hPSCs. Large cell colonies of hESCs, HUES8[19], and H9[1] were detached from fibronectin-coated dishes and dissociated into large cell clumps by incubation in PBS containing 1 mM Ca^{2+} without Mg^{2+} ($PBS^{ca/-}$) followed by pipetting (Supplementary Fig. 2a–g). These detached cell clumps were then plated into fibronectin-coated dishes and reattached as typical hPSC flat colonies on the next day (Supplementary Fig. 2h–m). In addition, hiPSCs cultured on vitronectin and laminin, which are also used as a coating matrix for culturing hPSCs (Table 1), can be detached from the culture dishes by $PBS^{ca/-}$ (Supplementary Fig. 3). These results suggested that enzyme-free solution containing physiological concentration of Ca^{2+}, but no Mg^{2+}, could be useful for passaging hPSCs as large cell clumps.

Effects of dissociation and enzymatic digestion. We compared our enzyme-free passage method to both dissociation passaging in a divalent cation-free solution and enzymatic digestion passaging.

Dissociating hPSCs into single cells and replating at low density causes cell damage and death by apoptosis[4–8]. Thus, we hypothesized that detaching and dissociating hPSCs into larger clumps using $PBS^{ca/-}$ could suppress apoptosis and support higher survival rates than detaching and dissociating these cells into smaller clumps using PBS without Ca^{2+} and without Mg^{2+} ($PBS^{-/-}$). To test this hypothesis, apoptosis was detected in the hiPSCs 253G1 and 201B7 using annexin V-FITC, which stains cell surface phosphatidylserine, four hours after detachment and dissociation in $PBS^{-/-}$ and $PBS^{ca/-}$ followed by floating culture in ESF9a solution. Fluorescence microscopy showed many annexin V-FITC-positive single cells dissociated by $PBS^{-/-}$, whereas annexin V-FITC-negative cells predominated in the large cell clumps dissociated by $PBS^{-/ca}$ (253G1: Fig. 2a, 201B7: Supplementary Fig. 4a). Quantitative analysis using flow cytometry (FCM) revealed that fewer annexin V-FITC-positive cells were detached and dissociated by $PBS^{ca/-}$ than by $PBS^{-/-}$, and that addition of a ROCK inhibitor (RI) abolished these differences (253G1: Fig. 2b, 201B7: Supplementary Fig. 4b). RI blocks the dissociation-induced apoptosis of hPSCs[6,7]. To measure cell survival, hPSCs were detached and dissociated in $PBS^{ca/-}$ or $PBS^{-/-}$, plated